Two-day wave coupling of the low-latitude atmosphere-ionosphere system

D. V. Pancheva,[1] P. J. Mukhtarov,[2] M. G. Shepherd,[3] N. J. Mitchell,[1] D. C. Fritts,[4] D. M. Riggin,[4] S. J. Franke,[5] P. P. Batista,[6] M. A. Abdu,[6] I. S. Batista,[6] B. R. Clemesha,[6] and T. Kikuchi[7]

Received 7 December 2005; revised 27 March 2006; accepted 12 April 2006; published 26 July 2006.

[1] Vertical coupling in the low-latitude atmosphere-ionosphere system driven by the 2-day wave in the tropical MLT region has been investigated. The problem is studied from an observational point of view. Three different types of data were analyzed in order to detect and extract the 2-day wave signals. The 2-day wave event during the period from 1 December 2002 to 28 February 2003 was identified in the neutral winds by radar measurements located at four tropical stations. The 2-day variations in the ionospheric electric currents (registered by perturbations in the geomagnetic field) and in the *F*-region electron densities were detected in the data from 23 magnetometer and seven ionosonde stations situated at low latitudes. Two features for each kind of wave were investigated in detail: the variation with time of the wave amplitude and the zonal wave number. The results show that the westward propagating global 2-day wave with zonal wave number 2 seen in the ionospheric currents and in *F*-region plasma is forced by the simultaneous 2-day wave activity in the MLT region. The main forcing agent in this atmosphere-ionosphere coupling seems to be the modulated tides, particularly the semidiurnal tide. This tide has a larger vertical wavelength than the diurnal tide and propagates well into the thermosphere. The parameter that appears to be affected, and thus drives the observed 2-day wave response of the ionosphere, is the dynamo electric field.

Citation: Pancheva, D. V., et al. (2006), Two-day wave coupling of the low-latitude atmosphere-ionosphere system, *J. Geophys. Res.*, *111*, A07313, doi:10.1029/2005JA011562.

1. Introduction

[2] The middle and upper atmosphere regions compose a strongly coupled system in which phenomena occurring at one height can have profound effects elsewhere. The mesosphere/lower thermosphere region (MLT) is a critical region in the vertical coupling since here physical processes filter and shape the flux of waves and tides ascending through the mesosphere into the overlaying thermosphere. The dynamics of the MLT region dominated by atmospheric tides, planetary, and gravity waves of large amplitudes determine to a great extend the wind system of the lower thermosphere. This wind system generates ionospheric electric fields and currents through the wind dynamo mechanism, as the electrically conducting medium is moved through the geomagnetic field. Both the winds and the electric fields produce plasma drifts that alter the ionospheric electron density distribution. Therefore the dynamo electric fields and currents produced by the interaction between the wind system and the ionospheric plasma control the quiet time electrodynamic processes of the low-latitude thermosphere-ionosphere system.

[3] If a global-scale wave with large amplitude and fairly long wavelength propagates from the MLT into the ionosphere, it should cause an electric current system to be driven with a period of the global-scale wave. This wave-like current system produces perturbations in the geomagnetic field that are easily measured at ground level. Then, the day-to-day variability in the ionospheric currents detected by ground-based magnetometer measurements, particularly during magnetically quiet conditions, could be due to penetration of planetary and gravity waves into the dynamo region or to short-term tidal variability with periods of planetary waves. Over the low-latitudes the Earth's magnetic field lines are almost horizontally oriented and this leads to a condition in which the dynamo electric fields generated by the global-scale waves play a leading role in the associated response of the ionosphere *F*-region. *Forbes and Leveroni* [1992] found a quasi 16-day oscillation in the *E*- and *F*-regions of the equatorial ionosphere during

[1]Centre for Space, Atmospheric, and Oceanic Sciences, Department of Electronic and Electrical Engineering, University of Bath, Bath, UK.
[2]Geophysical Institute, Bulgarian Academy of Science, Sofia, Bulgaria.
[3]Centre for Research in Earth and Space Science, York University, Toronto, Ontario, Canada.
[4]Colorado Research Associates, Division of NorthWest Research Associates, Boulder, Colorado, USA.
[5]Department of Electrical and Computer Engineering, University of Illinois at Urbana-Champaign, Urbana, Illinois, USA.
[6]National Institute for Space Research, São José dos Campos, Sao Paolo, Brazil.
[7]Solar-Terrestrial Environment Laboratory, Nagoya University, Nagoya, Japan.

0148-0227/06/2005JA011562

Table 1. Geographic Locations of the MLT Radars and Periods of Measurements

Station	Instrument	Location	Period of Measurements	Height Range
Maui, Hawaii	Meteor radar	20.8°N, 156.2°W	01 Dec–28 Feb	81–99
Rarotonga	MF radar	21.2°S, 159.8°W	02 Dec–20 Jan	82–98
Rarotonga	Meteor radar	21.2°S, 159.8°W	23 Jan–28 Feb	82–98
Cachoeira Paulista	Meteor radar	22.7°S, 45°W	03 Dec–28 Feb	81–99
Ascension Island	Meteor radar	7.9°S, 14.4°W	13 Jan–17 Feb	81–97

January/February 1979, likely connected with the upward penetration of a free Rossby mode excited in the winter stratosphere. The wave signatures in the equatorial electrojet over Huancayo, Peru, analyzed by *Parish et al.* [1994] for an interval from early 1979 to the end of 1986 indicated that 2-, 5-, 10- and 16-day periodicities have significant amplitudes and are found to persist with nearly constant periods for intervals of days to weeks. They attributed these periodicities to the planetary waves; however, their analysis suggested also that nonlinear interactions between the planetary waves and the diurnal and semidiurnal tides could be another driving source of these oscillations. There has been further recent interest in planetary wave forcing of the equatorial ionosphere leading to new observational studies by *Takahashi et al.* [2005], *Ramkumar et al.* [2005], *Abdu et al.* [2006], and the review paper by *Lastovicka* [2006].

[4] The quasi-2-day wave is a predominant feature of the tropical MLT region during January and early February each year with amplitude frequently exceeding 50–60 m/s. *Ito et al.* [1986] first theoretically suggested that a large-amplitude global-scale 2-day wave can induce an electric current system in the ionosphere through a dynamo mechanism. *Takeda and Yamada* [1989], *Rangarajan* [1994], and *Yamada* [2002] detected quasi-2-day variability in geomagnetic field and discussed its possible relationship with the 2-day wave in the atmosphere; however, no wind measurements supported their results. *Gurubaran et al.* [2001a] identified the signatures of the quasi-2-day variability in the equatorial electrojet and showed a reasonable correlation with the 2-day wave measured by the MF radar situated close to the geomagnetic stations. *Parkinson* [1982], however, in an attempt to isolate 2-day signal from the variability of the geomagnetic field, concluded that the mesospheric winds did not cause detectable geomagnetic effects. In addition, simulation studies of the quasi-2-day wave by *Hagan et al.* [1993] indicated that the oscillation is extremely sensitive to the zonal mean winds and the inclusion of a realistic stratospheric jet is accompanied by a reduction of 2-day wave amplitudes above 100-km altitudes. Despite of many observations reporting quasi-2-day signatures in the ionosphere [*Pancheva and Lysenko*, 1988; *Chen*, 1992; *Pancheva et al.*, 1994; *Apostolov et al.*, 1995; *Forbes et al.*, 1997; *Altadill and Apostolov*, 1998], the forcing of the ionosphere, and in particular the electric fields and currents above 100-km altitudes by the 2-day wave observed in the MLT region, remains an open problem.

[5] The aim of this work is to investigate the quasi-2-day variability in the ionospheric electric currents (detected by ground-based magnetometer measurements) and in the maximum electron density of the ionosphere *F*-region at low latitudes possibly forced by a 2-day wave present in the MLT region. Three different types of data are analysed to detect and extract the 2-day wave signals present simultaneously in: (1) the neutral winds, (2) the geomagnetic fields, and (3) the critical plasma frequency (*foF2*) of the ionosphere F-region. The 2-day wave events are identified in the neutral winds measured by radars located at four tropical stations. The 2-day variations in the ionospheric electric currents and *F*-region electron densities were detected in the data from 23 magnetometer and seven ionosonde stations situated at low latitudes (from 30°N to 30°S). Our study focuses on the interval from 1 December 2002 to 28 February 2003. Our intent is to look for correlations between the 2-day wave in the MLT winds and the 2-day variability in the geomagnetic field and *foF2* in order to evaluate whether these three oscillations are interrelated. Two properties are investigated for each data set: the variation with time of the wave amplitude and the zonal wave number.

2. Quasi-2-Day Wave in the Tropical MLT Region

[6] It is known that the quasi-2-day wave can attain large amplitudes, as large as 80–90 m/s, particularly in the meridional wind component of the equatorial MLT region. That is why the global features of the 2-day wave during December 2002 to February 2003 are investigated using only meridional wind measurements at four stations: Maui, Rarotonga, Cachoeira Paulista, and Ascension Island. Table 1 lists the radar locations, type, and available data. We note that the 2-day wave activity over Rarotonga is identified by combined measurements made by MF radar between 2 December 2002 and 20 January 2003 and later by meteor radar which began regular observations on 23 January 2003. The data from Ascension Island are used as supplementary measurements because they cover only part of the investigated time interval, or 13 January to 17 February 2003. The waves studied in this paper were found to be highly dynamic with amplitude and phase changes over relatively short timescales. A detailed description of the methods used for analysis of such waves can be found in the work of *Pancheva et al.* [2004a, 2004b]. A Morlet wavelet transform was performed on the hourly mean data in order to investigate the temporal behavior of the quasi-2-day wave. The wavelet spectra were calculated in the period interval between 4 and 96 hours. Figure 1 shows the wavelet spectra at 90 km altitude for the four stations and the basic features of the 2-day wave event can be summarized as follows: (1) the 2-day wave appears in late December (around 25 December), peaks at most of the stations between 10 and 25 January, and persists until early February (it disappears around day number 70); actually, the 2-day wave over Maui and Rarotonga disappears a few days earlier than that over Cachoeira Paulista and Ascension Island, (2) the 2-day wave activity consists of several bursts with periodicity of 6–8 days, (3) the largest amplitudes at

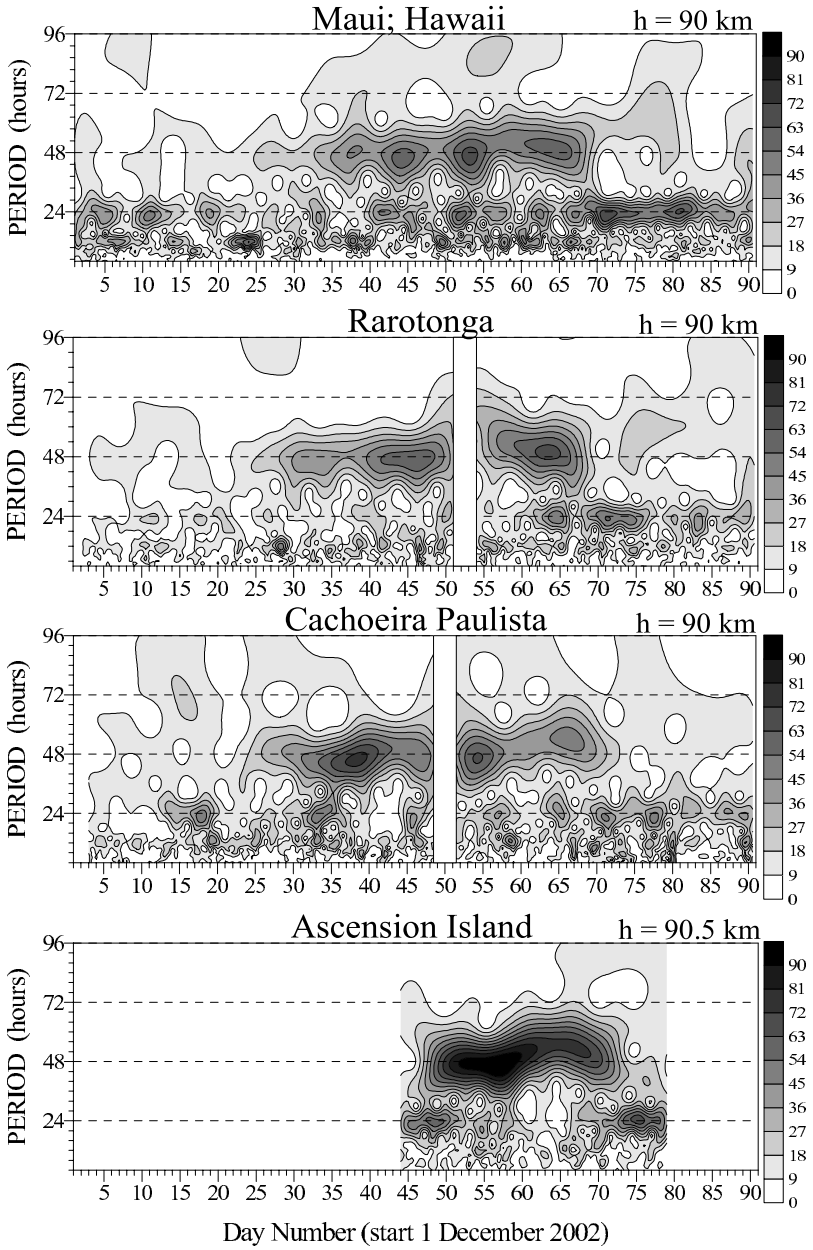

Figure 1. Wavelet spectra of the meridional wind at 90 km height calculated for periods between 4 and 96 hours for the stations Maui, Rarotonga, Cachoeira Paulista, and Ascension Island.

90 km height reach 70–80 m/s over Maui, Rarotonga, and Cachoeira Paulista, whereas those over Ascension Island reach 90–100 m/s, (4) the 2-day wave events are not coherent among sites, which may be an indication that zonal wave number 3 not be solely contributing (as is usual for the 2-day wave in boreal winter) contributing to the 2-day wave events, and (5) an anticorrelation between the occurrence of maximum 2-day wave and the diurnal tidal activity is observed. The last interesting feature is not newly discovered, but was reported earlier by *Harris and Vincent* [1993], *Gurubaran et al.* [2001b], and *Pancheva et al.* [2004a, 2004b].

[7] The 2-day wave itself was studied using two methods: a complex demodulation method [*Bloomfield*, 1976] and a least squares best-fit method. The 2-day wave characteristics obtained by both methods were very similar. Figure 2 shows the time-height cross section of the amplitudes (left column of plots) and phases (right column) of the quasi-2-day wave. The wave characteristics in the plots are obtained with the complex demodulation method, so the phases are in radians. In this case a 48-hour demodulation period and an effective bandpass filter with 3-db points at 40 and 60 hours were used. The burst-like character of the 2-day event is clearly outlined in the 2-day wave amplitude plots. Most of the bursts maximize around 90 km; however, there is a tendency for the amplitudes to maximize at increasing altitudes after the middle of January (this is not clear only at Cachoeira Paulista). The phase slopes, negative at the beginning and positive at the end of the 2-day wave event, are similar at all stations (right column of plots). This means

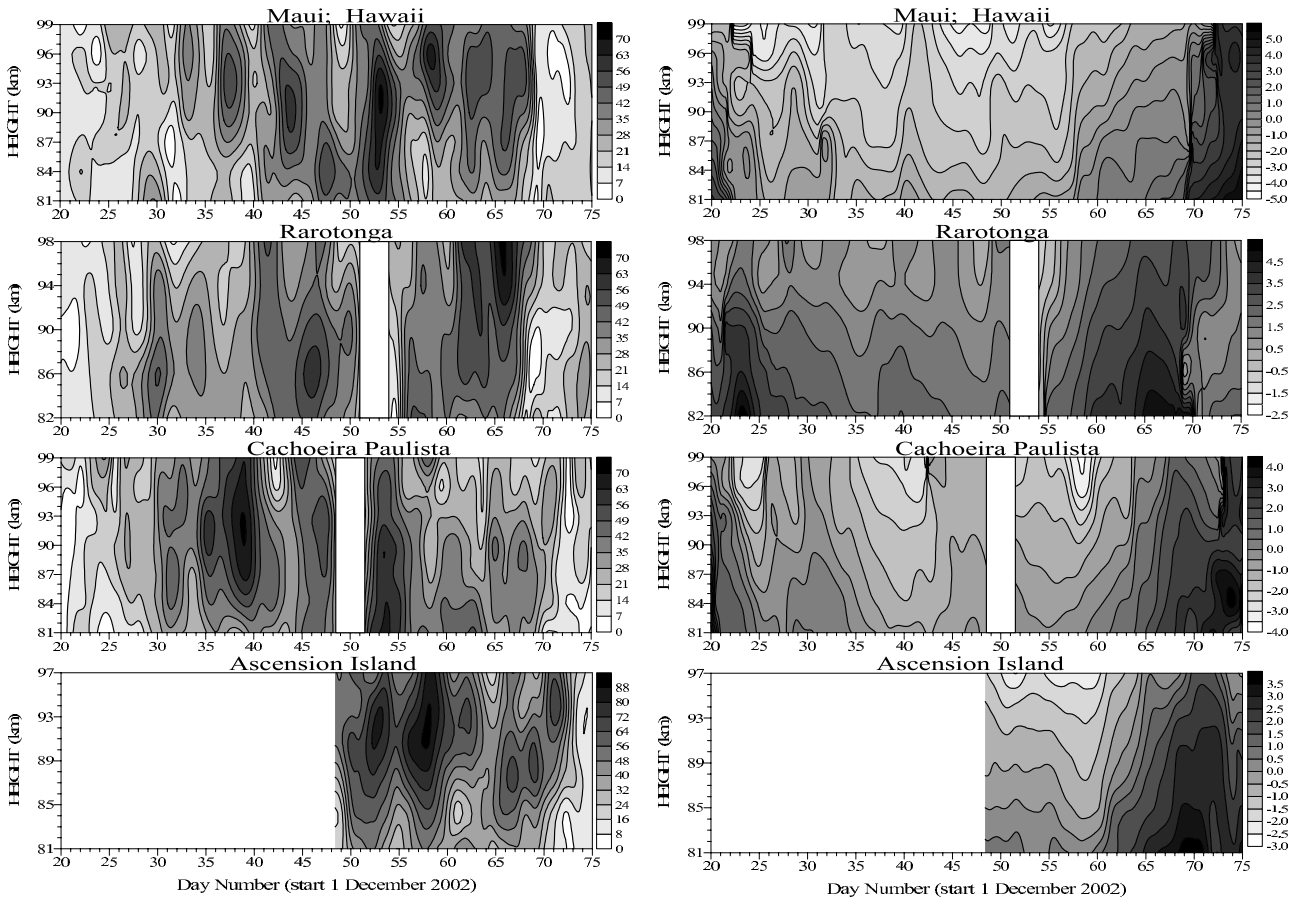

Figure 2. Time-height cross sections of the amplitudes (left column of plots) and phases (right column) of the quasi-2-day wave for all stations. The wave characteristics are obtained by complex demodulation method (for details see text); the wave amplitude is measured in m/s, while the phase is measured in radians.

that the period of the quasi-2-day wave changes during the time of observations, but these changes are similar at all stations. The short-term variability of the phases that result from the burst-like character of the 2-day wave events can be distinguished in the phase plots as well. The vertical wavelengths of the 2-day wave calculated for all stations are not very different and range between 50 and 65 km.

[8] An important characteristic of the waves is their direction of propagation and the zonal structure (zonal wave number). For this purpose we can use only data from the three stations situated in the Southern Hemisphere (SH). Two of them, Rarotonga and Cachoeira Paulista, are particularly useful because they are located at almost the same latitudes (21–22°S), while Ascension Island is too close to the equator (7.9°S). As was mentioned before, the period of the 2-day wave changes during the observations. Therefore it is better to apply a cross wavelet analysis, which gives local information about the simultaneous presence of the 2-day wave with similar periods at two stations and the phase difference between them. The upper plot of Figure 3 shows the cross wavelet power between the 2-day wave observed at Cachoeira Paulista and Rarotonga. The burst-like character is clear in the cross wavelet power plot. The middle plot of Figure 3 indicates the zonal wave number calculated from the phase difference between the two stations. On the basis of data only from these two stations we may conclude that the 2-day wave propagates westward with primary zonal wave number 2 in the first time interval (from the beginning of the 2-day wave activity to the middle of January) and with primary zonal wave number 3 after 23 January. The data from Ascension Island can be used only for clarifying the wave number in the second interval. Unfortunately, data from the three stations suggested no definitive wave number and a potential for a superposition of zonal wave numbers 2 and 3. There are two possible reasons which could explain why we were unable to find a definitive wave number:

[9] 1. The 2-day wave in December 2002 to February 2003 might not have a zonal wave number 3 (as is usual for the 2-day wave in boreal winter) because it can differ from the pure Rossby-gravity (3,0) mode. It is known that for the (3,0) mode the meridional wind should be in phase, while the zonal wind should be out of phase. The phase profiles of the 2-day wave in the meridional and zonal winds at Maui and Rarotonga, which are symmetrical stations with respect to the equator, do not support this requirement. The bottom plot in Figure 3 shows the 2-day wave phases (in UT) in meridional wind at 90 km height for Maui (solid line) and Rarotonga (dash line); the phase difference is ~18 hours. Similarly, the phase difference in the zonal wind was found

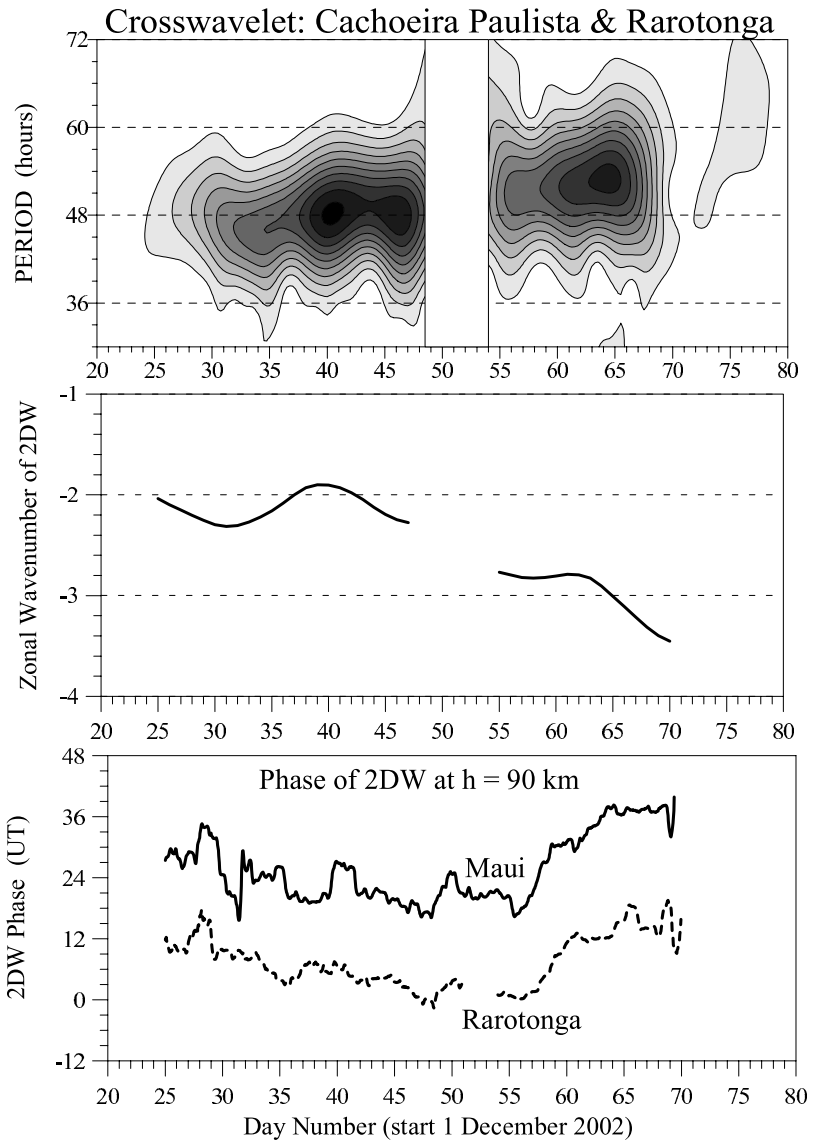

Figure 3. Cross wavelet power spectrum between the 2-day wave observed at Cachoeira Paulista and Rarotonga (upper plot). Zonal wave number calculated from the phase difference between the 2-day wave observed at Cachoeira Paulista and Rarotonga (middle plot). The 2-day wave phases (in UT) in meridional wind at 90 km height for Maui (solid line) and Rarotonga (dashed line) (bottom figure).

to be ~7 hours (not shown here). Therefore the 2-day wave event in December 2002 to February 2003 is characterized by a steep latitudinal phase slope and this feature hampers the wave number determination using stations located at different latitudes.

[10] 2. The burst-like character of the 2-day wave event complicated the analysis as well. It was found that the 2-day amplitudes were strongly modulated at planetary wave periods of 6–8 days and that coupling between the planetary waves with different periods may also have influences on 2-day wave phases as well.

3. Two-Day Variability Observed in the Magnetometer Data

[11] Hourly geomagnetic data were obtained for 23 stations from the World Data Centre (WDC) for Geomagnetism, Denmark, and the WDC, Boulder, Colo. The selected stations are listed in Table 2 together with their geographic and geomagnetic coordinates (the geomagnetic coordinates were calculated by the Geomagnetic Coordinates Program GMCORD downloaded from the WDC, Boulder) and the percentage of valid data. It should be noted that the geomagnetic components stored in the WDC and used in this analysis differ between stations; some of the sites are archived as H, D, and Z components oriented with respect to the geomagnetic field, and the others are archived as X, Y, and Z components oriented with respect to the geographic pole. The H and D components recorded for those stations were converted to X and Y components.

[12] It is important to note that the amplitude of the perturbation detected in the geomagnetic signal is not only dependent on the magnitude of the neutral wind perturbation in the dynamo region but is also dependent on the

Table 2. Geographic and Geomagnetic Coordinates of the Magnetometer Stations and the Percentage of Valid Data

Code	Latitude	Longitude	MLAT	MLONG	Valid Data
AAE	9.03	38.76	5.02	112.4	99.75%
ABG	18.64	72.87	9.75	146.7	98.52%
BNG	4.33	18.57	4.09	91.7	89.12%
GUA	13.58	144.87	4.96	216.1	94.55%
HON	21.32	202	21.73	270.1	99.97%
HUA	−12.05	284.67	−1.34	357	100.00%
KDU	−12.68	132.47	−22.37	206.2	100.00%
KOU	5.1	307.4	15.18	307.4	100.00%
PPT	−17.57	210.42	−14.92	285.8	99.12%
SJG	18.12	293.85	28.78	6.7	98.89%
TND	1.29	124.95	−8.95	197.5	98.84%
DLR	29.43	259.08	38.69	327.7	99.95%
TEO	19.75	260.81	29.23	330.8	97.96%
PHU	21.03	105.97	10.31	178.4	100.00%
SLZ	−2.58	315.77	0.04	29.8	84.54%
API	−13.8	188.22	−15.39	262.9	65.09%
CTA	−20.08	146.25	−28.32	221.2	100.00%
GUI	28.32	343.56	33.97	61	85.00%
HBK	−25.88	27.71	−27.18	94.3	97.31%
LRM	−22.2	114.1	−32.82	186.6	96.76%
TAM	22.79	5.53	24.7	82.1	98.94%
TAN	−18.92	47.55	−23.88	115.7	71.00%
VSS	−22.4	316.35	−12.91	26.7	94.72%

conductivity. This conductivity will change not only between day and night conditions or over the course of a solar cycle [*Takeda et al.*, 2003], but during geomagnetic storms and due to precipitation of charged particles from the magnetosphere. In addition, during magnetic storms two main physical processes acting on a planetary scale can be observed: (1) the direct penetration of polar cap electric fields to the equator [*Nishida*, 1968; *Kikuchi et al.*, 1996] and (2) the disturbance of winds due to auroral Joule heating and ion-drag acceleration [*Blanc and Richmond*, 1980; *Richmond*, 1995]. Therefore we should expect the magnetic storm effects in the geomagnetic components to be present as well.

[13] Figure 4 shows the wavelet spectra of the 3-hourly geomagnetic a_p-index and the hourly equatorial D_{st}-index for the period of December 2002 to February 2003. The vertical thick lines on both plots outline the interval when the 2-day wave event is present in the MLT region. Two disturbed intervals can be easily distinguished: around 18–23 December and 2–4 February. The first geomagnetic disturbance is outside of the time interval of interest; however, the second geomagnetic disturbance is inside it. This means that if we observe the 2-day variations in the geomagnetic or ionospheric data after 1 February they should be affected by the geomagnetic storm as well.

3.1. Data Analysis Method

[14] Figure 5 shows some examples of spectra obtained by the correloperiodogram analysis performed on the raw hourly geomagnetic data. This was done to see if there was some power at periods near 48 hours, knowing in advance that it should be small as the components of the quiet-day geomagnetic perturbations, commonly labeled as *Sq* (for "solar quiet"), typically dominate the spectrum. The spectral results in Figure 5 show that some 2-day variability in the geomagnetic components is indeed present. The main purpose of this work, however, is not only to detect the 2-day geomagnetic variations but also to extract and study them in detail. Hence an important step is the choice of a method for extracting the 2-day variations from the hourly data.

[15] We now describe a novel method of analysis that is based on the observational evidence that the 2-day variability in the geomagnetic components appears as modulation of the quiet-day (normal) *Sq* diurnal cycle. A careful inspection of the raw data indicates that during periods when the 2-day variations are present the diurnal cycle is significantly distorted. The upper row of plots in Figures 6 shows two examples of raw hourly data (Y and Z components) when the 2-day variations are present in the data. The plots show not only that the diurnal cycles are distorted from normal ones but also that they are inverted every second day. In order to distinguish the intervals with modulated (or distorted) diurnal cycles, supposing that they are related to the 2-day variations, we first have to define the normal (undisturbed) diurnal cycle for each station. We accepted the mean diurnal cycle for the entire 3-month interval to represent the normal diurnal cycle, which is marked as $R_m(UT)$, where with R is denoted the X-, Y-, or Z-component and UT = 0,1,.....,23. We note also that the daily mean values are not important in this study because we are interested in the modulated diurnal cycles. This means that we will work with a mean diurnal cycle with daily mean removed in advance, which is marked as $dR_m(UT)$. This diurnal cycle is used as a benchmark for departures due to 2-day wave modulation. The middle row of plots in Figure 6 shows the mean diurnal cycles for the examples under consideration. Then each 24-hour segment centered at the time t and covering the time moments: $vt = t - 11,\ t - 10,\ldots,t,\ldots,t + 12$ with a sliding daily mean removed in advance, $R_0(t)$, can be expressed as:

$$dR(vt) = R(vt) - R_0(t) \tag{1}$$

In order to compare each diurnal cycle, described by (1), with the benchmark $dR_m(vt)$, we perform a sliding linear regression using a 24-hour segment and a sliding step of

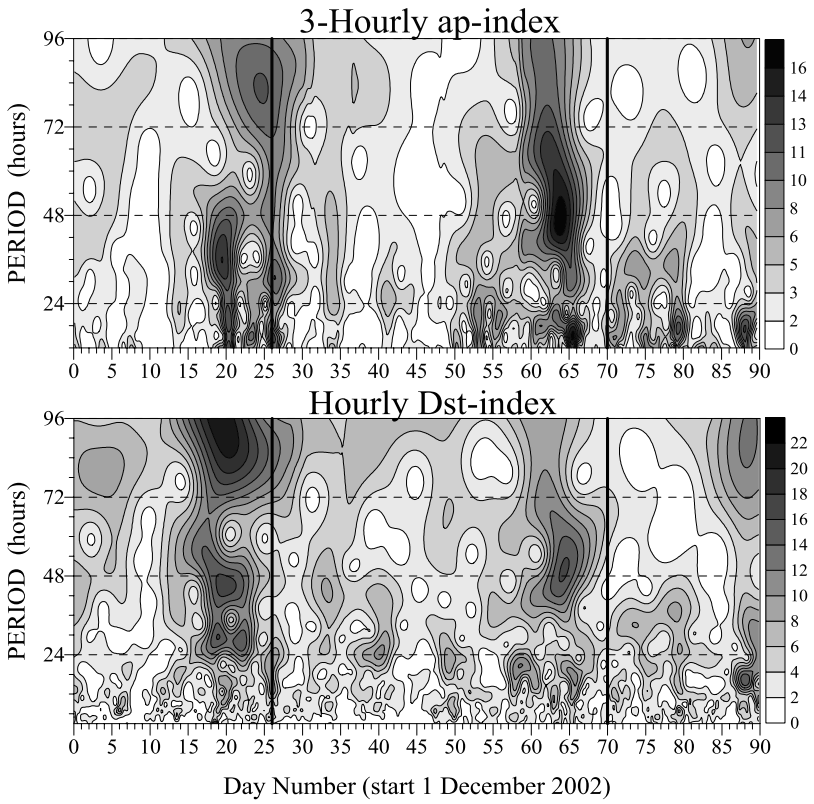

Figure 4. Wavelet spectra of the 3-hourly geomagnetic a_p-index (upper plot) and the hourly equatorial D_{st}-index (bottom plot) for the period of December 2002 to February 2003. The vertical thick lines on both plots outline the time period when the 2-day wave event is present in the MLT region.

1 hour. The regression coefficients $M_s(t)$ and $M_0(t)$ are found by a least squares best-fit method from the relation:

$$dR(vt) \approx M_s(t) dR_m(vt) + M_0(t) \tag{2}$$

Actually, the values of $M_0(t)$ are very small because we removed in advance the daily means. The coefficients $M_s(t)$ serve as a scale factor and they define the scope of change of a particular diurnal cycle with respect to the mean diurnal one for the studied time interval. We will work with the relative scale coefficient representing the linear regression between $dR(vt) - dR_m(vt)$ and $dR_m(vt)$ because the time series of this parameter have zero mean. It is defined by

$$M_{sr}(t) = M_s(t) - 1 \tag{3}$$

The bottom row of plots in Figure 6 shows the time series of the relative scale coefficients for the *Y*- and *Z*-components of the two stations considered and obtained by applying the above described procedure on the raw hourly data. The 2-day variations can be distinguished easily by eye.

[16] We note that using time series of $M_{sr}(t)$ means that the 24-hour periodicity together with all harmonics are removed in advance. This method represents a special single-component decomposition of data, where instead of using a standard sine function we use a concrete diurnal course, which is treated as periodic, but which is not a simple sinusoid.

3.2. Results

[17] The hourly *X*, *Y*, and *Z* component data from all 23 stations were processed by the procedure described above and the $M_{sr}(t)$ coefficient time series have been analyzed by standard spectral methods. First, we investigated which of the prevailing periods of the 2-day wave were present in the scale coefficient time series. It was found that in the *Y* and *Z* components all stations show strong peaks clustered near 48 hours and only several of them indicate secondary peaks near 55–57 hours but with amplitudes almost two times smaller than those near 48 hours. The similar result was obtained for the *X* component; however, the secondary peaks near 55 hours were larger, on the average ~75–80% of those near 48 hours. As the main peaks for *X*, *Y*, and *Z* components for all stations were clustered near 48 hours that is why the amplitudes and phases of the 2-day geomagnetic variations were retrieved by a least mean squares procedure assuming that the period of the 2-day wave is 48 hours. The 2-day amplitudes and phases were determined in segments of 48-hour duration and segments were incremented through the time series in steps of 1 hour yielding time series of hourly spaced values.

[18] The least mean squares method works generally with unevenly distributed data or in this case particularly with data gaps. Table 2 gives information about the percentage of the gaps for each station. We used the following criteria for

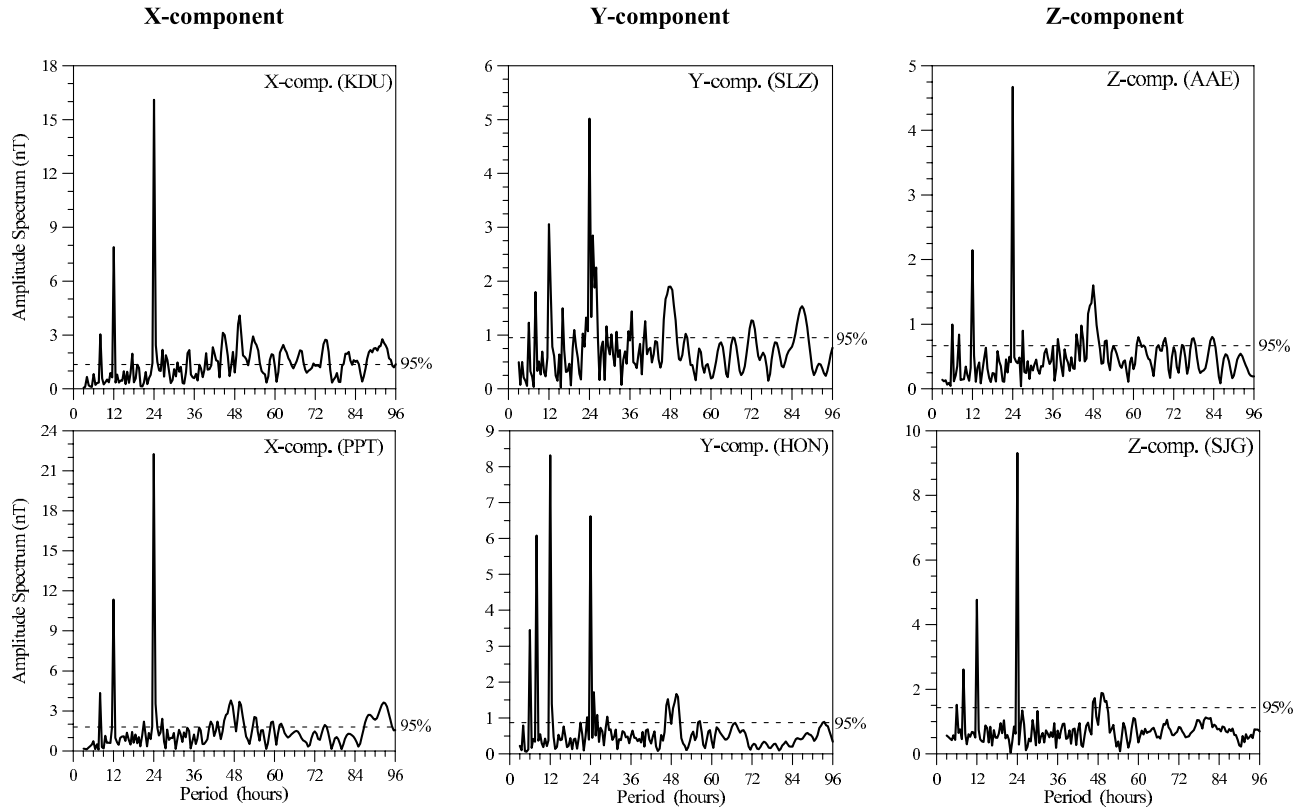

Figure 5. Amplitude spectra obtained by the correloperiodogram analysis and performed on the raw hourly geomagnetic data for *X*-component (left column), *Y*-component (middle column), and *Z*-component (right column).

obtaining a stable solution: the number of gaps in a 48-hour window should be not larger than 24 and the length of the largest successive gap to be not longer than 12 hours. If this condition was violated for a concrete hour then there were no assigned an amplitude and phase of the 2-day wave for this hour.

[19] We investigate separately the stations from the Northern Hemisphere (NH) (13 stations) and from the Southern Hemisphere (SH) (10 stations), with the goal of defining the variability of the two current vortices situated in the two hemispheres. Figure 7 shows the time-longitude surfaces of the amplitudes of 2-day variability observed in the *X* component (left column), in the *Y* component (middle column), and in the *Z* component (right column) separately for the NH (upper plots) and the SH (lower plots). The basic features evident in this figure can be summarized as follows:

[20] 1. *X* component: (1) in general, the 2-day variability in this component was strongly affected by the two geomagnetic disturbances centered at day numbers 20 and 65, (2) however, there were intervals, namely, between day numbers 30–40 and 50–60, when the 2–day variations were present at many stations and these 2-day variations should be attributed to the 2-day wave observed in the tropical MLT region, and (3) significant longitudinal differences of the 2-day geomagnetic variations occurred in the SH and were stronger in the eastern part of the SH.

[21] 2. *Y* component: (1) the 2-day variability in this component amplified mainly when the 2-day wave event was present in the MLT region, between day numbers 26 and 70 (see the marked interval in Figure 4), (2) there were two clearly defined periods when 2-day variations were strong at most of the magnetometer stations; these periods coincided with the initial (late December early January) and final (late January early February) stages of the 2-day activity in the MLT region, and (3) longitudinal differences were particularly visible in the SH, and the 2-day variations were stronger in the western part of the SH.

[22] 3. *Z* component: (1) the 2-day variability of this component amplified predominantly when the 2-day wave event was present in the MLT region, however, the effect of the two geomagnetic disturbances was apparent as well, and (2) similarly to the *Y*-component, the 2-day variations in *Z*-component achieved large amplitudes at most stations from late December to early January and again from late January to early February, or during the initial and final stages of the 2-day wave activity in the MLT region.

[23] The 23 magnetometer stations used in this study were well distributed longitudinally and this enabled us to study the zonal structure of the 2-day variations observed in the geomagnetic components. Specifically, we investigated whether the 2-day variations of the geomagnetic components were fluctuations of unknown origin or whether they represented a zonally propagating wave. For this purpose two periods, 26 December 2002 to 5 January 2003 and 20 January to 1 February 2003, during which the 2-day amplitude increased at most stations, were examined in detail. For each station and for each period we performed

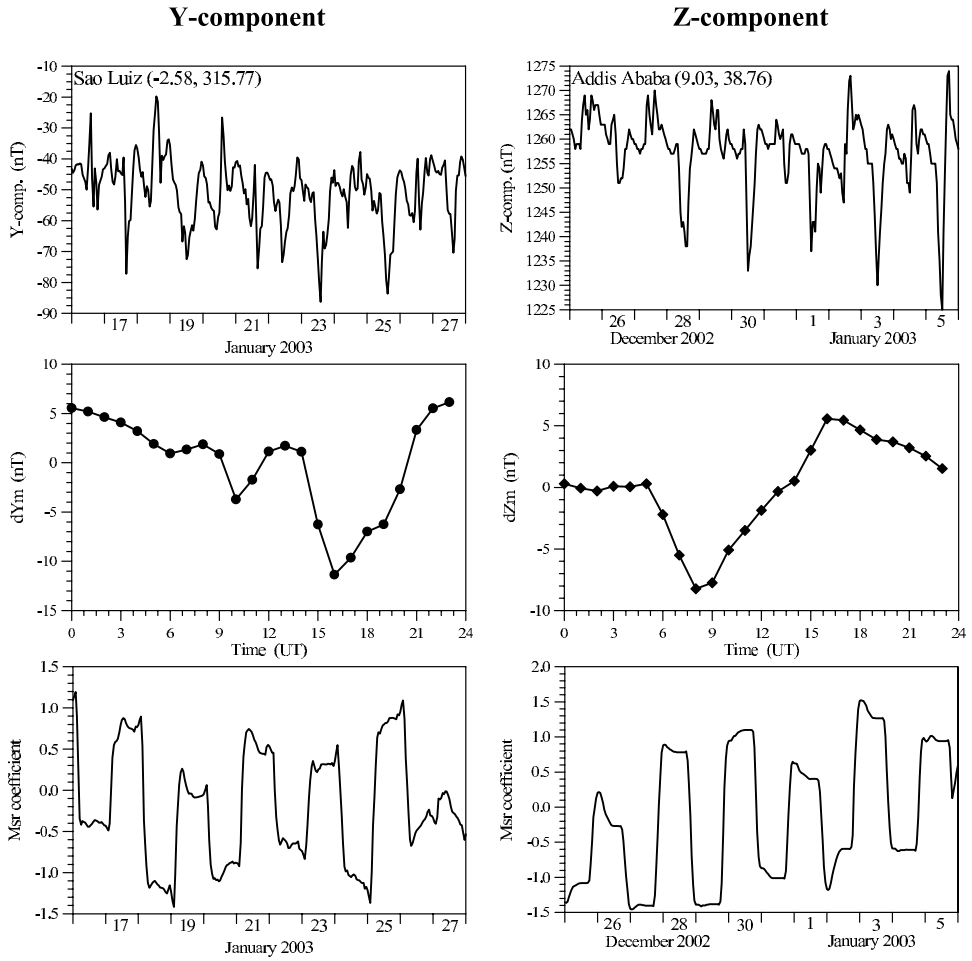

Figure 6. Two examples of raw hourly data (*Y*- and *Z*-components) when the 2-day variations persist in the data (upper row of plots). The mean diurnal cycles for both examples (middle row of plots). The time series of the relative scale coefficients for the *Y*- and *Z*-components of the two examples (bottom row of plots).

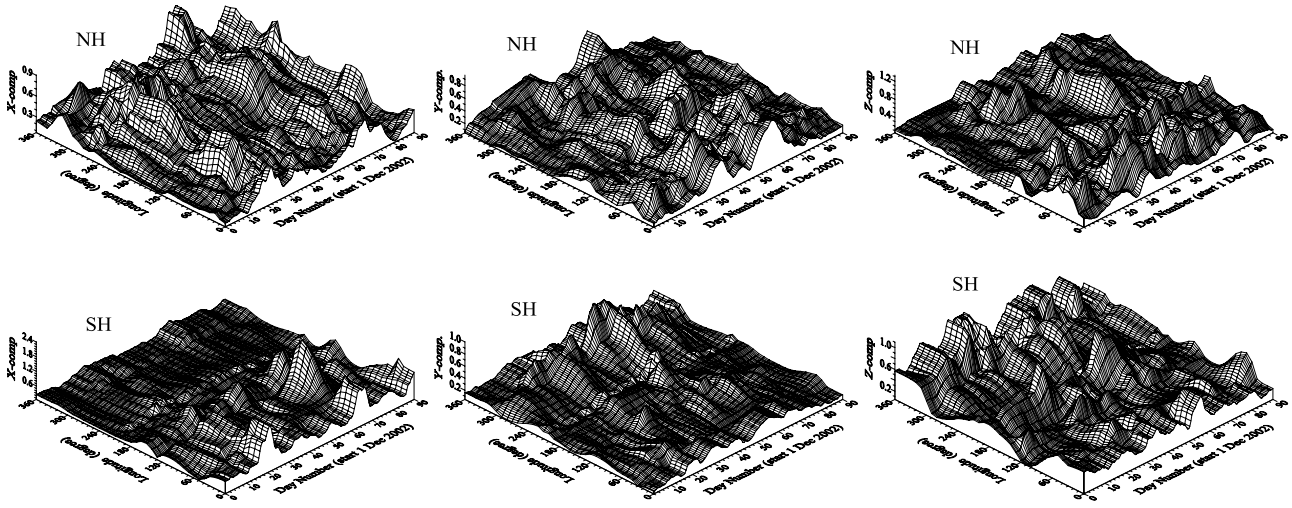

Figure 7. Time-longitude surfaces of the amplitudes of 2-day variability observed in *X*-component (left column), in *Y*-component (middle column), and in *Z*-component (right column) respectively for NH (upper row of plots)) and SH (bottom row of plots).

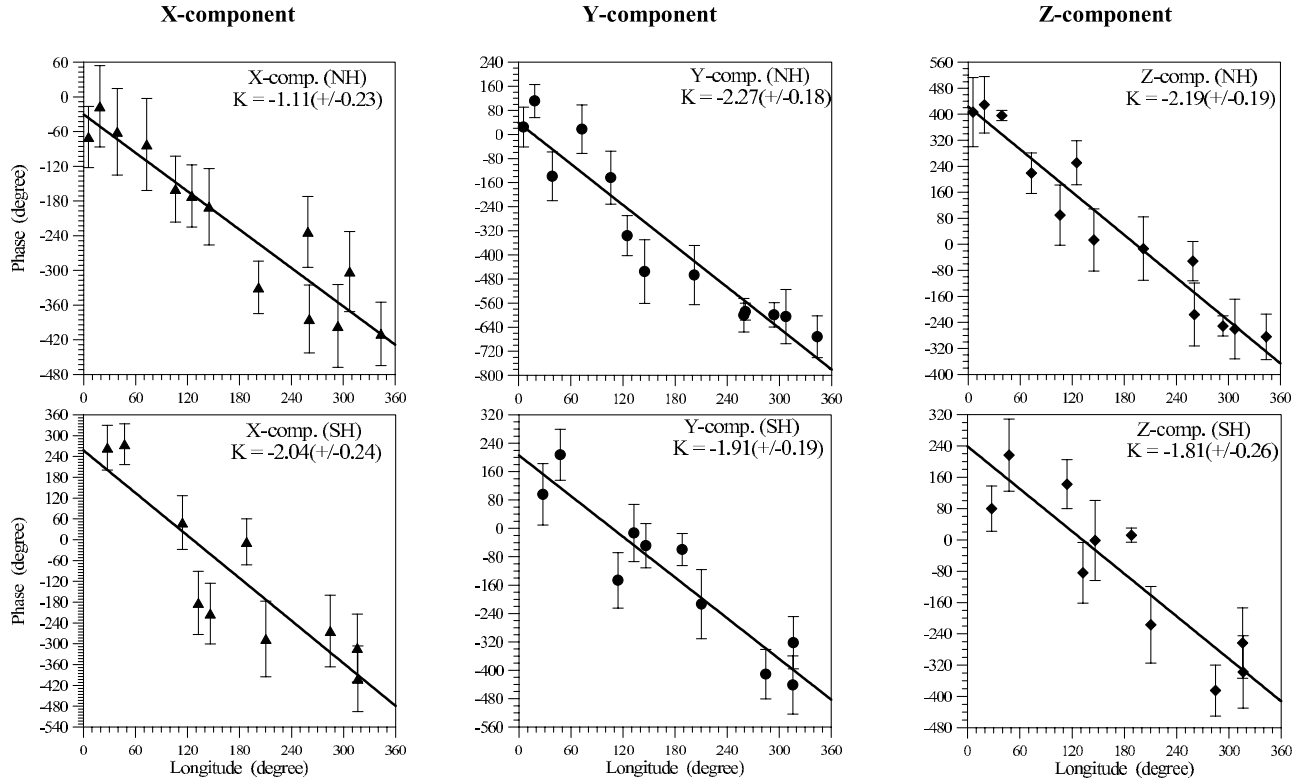

Figure 8. Phase slopes found in the relative scale coefficients of *X*-component (left column), of *Y*-component (middle column), and of *Z*-component (right column) for the period of 26 December 2002 to 5 January 2003 separately for the NH (upper row of plots) and for the SH (bottom row of plots).

a vector averaging of the amplitudes and phases to obtain the mean amplitude and phase of the 2-day wave. This defined the longitudinal distributions of these quantities. Figure 8 shows the phase slopes found in the relative scale coefficients of the *X* component (left column), *Y* component (middle column), and *Z* component (right column) for the first period in the NH (upper row of plots) and for the SH (bottom row of plots), respectively. The longitudinal distribution of the phases for *Y* and *Z* components for both hemispheres reveals a westward propagating 2-day wave response with primary zonal wave number 2 (W2). The longitudinal distribution of the phases for the *X* component, however, reveals a westward propagating 2-day wave response with primary zonal wave number 1 (W1) in the NH and 2 (W2) in the SH. Figure 9 shows the longitudinal distribution of the phase slopes, but for the second period, 20 January to 1 February 2003. Again, the longitudinal distribution of the phases for *Y* and *Z* components for both hemispheres reveals a westward propagating 2-day wave response with primary zonal wave number 2 (W2), while for *X* component exhibited a primary zonal wave number between 1 and 2 in the NH and 1 (W1) in the SH.

[24] The detailed amplitude and phase analysis of the 2-day variations in the geomagnetic components indicated some differences in their response to the 2-day wave activity in the MLT region and to the geomagnetic disturbances with similar timescales. The 2-day wave response in all components represents a W2 wave for *Y* and *Z* components, but W1 and W2 waves for the *X* component. The amplitudes of the 2-day variations in the *X* component are strongly affected by the geomagnetic disturbances, while those in the *Y* component are amplified during the 2-day wave activity in the MLT region and are almost unaffected (particularly in the NH) by the geomagnetic disturbances.

3.3. Global-Scale Amplitudes of the 2-Day Wave in the Geomagnetic Components

[25] The apparently reliable estimates for the zonal wave numbers of the 2-day wave geomagnetic response in both hemispheres have been used as a basis for performing a two-dimensional (2-D, time-longitude) Fourier transform. In this way the global 2-day wave response of the geomagnetic components can be represented more clearly. It has been done by using the formula:

$$M_{sr} = M_{sr0} + \sum_{k=1}^{2} M_{srk} \cos\left(\frac{2\pi}{48} t + \frac{2\pi}{360}(kl - \Phi_k)\right) \qquad (4)$$

where l is longitude and M_{srk} and Φ_k are the amplitude and phase of the W1 and W2 waves. The 2-D Fourier transform was performed using a 48-hour segment, with this segment then incremented through the time series in steps of 1 hour. Thus the global 2-day wave observed in each geomagnetic component during the interval December 2002 to February 2003 was described by its hourly (instantaneous) amplitudes and phases (phases are not shown here). We remind the reader that the 2-day wave response of the *Y* and *Z* components in both hemispheres is composed only of one W2 wave, while that of the *X* component is composed of

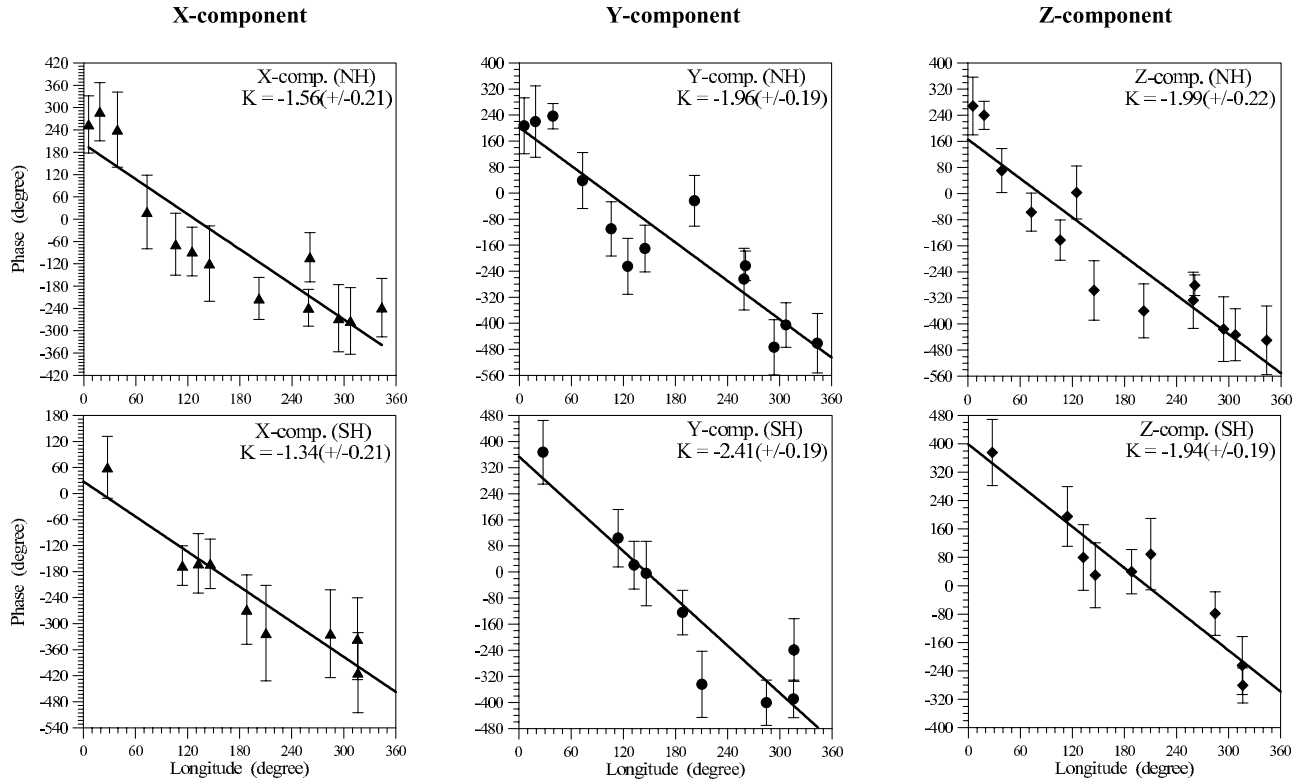

Figure 9. Same as in Figure 8, but for the period of 20 January to 1 February 2003.

two W1 and W2 waves. The instantaneous amplitudes of the global 2-day wave in all geomagnetic components and for the NH are shown in the left column in Figure 10, while those for the SH are shown in the right column. In general, the amplitudes of the global 2-day wave in all components and in both hemispheres are highly variable, but we note that the 2-day wave event in the MLT region was highly variable as well (see Figure 2).

[26] The amplitudes of the global 2-day W1 wave (solid line) and W2 wave (dash line) in the *X* component are shown in the upper row of Figure 10. It is clearly that W2 wave is significantly weaker than W1. The largest peaks marked by arrows in the figure are those related to the geomagnetic disturbances. Therefore the 2-day wave response of the *X* component was strongly determined by the two geomagnetic disturbances with timescales around 2 days (see Figure 4). The response of the *X* component to the geomagnetic disturbances was not a surprise to us, but the wave number 1 was not anticipated. We expected predominantly symmetrical responses to the geomagnetic disturbances. That is why a 2-D Fourier transform was performed again with a further addition of a new wave with zonal wave number 0 (W0). This was done with hope that W0 wave would maximize around day numbers 20 and 65 (when the geomagnetic storms took place) and would weaken significantly the W1 wave by extracting energy from it. The result, however, was completely different; W0 proved to be very weak, while the W1 was almost unaffected by adding the additional wave (the result not shown here). Hence the response of the *X* component can be described mainly by the W1 wave. A possible reason for this result may be in the opposite reactions of the daytime and nighttime parts of the ionosphere to the geomagnetic disturbances.

[27] The amplitudes of the global 2-day W2 wave in the *Y* component for both hemispheres are shown in the middle row in Figure 10. The amplification of the global 2-day W2 wave coincides with the 2-day wave event in the MLT region (between day numbers 26 and 70). However, the amplitudes are largest at the initial and final stages of the 2-day wave event, when the 2-day wave amplitudes are not as large. The latter is clearly defined in the NH, while the initial maximum of the global 2-day wave in the SH is present, but is weaker than the final one. It should be mentioned, that the result for the SH could be partly related to the smaller number of stations (compared to NH) used for the 2-D Fourier transform; we used data from only 10 stations in the SH (as opposed to 13 for NH) and a few of them have quite spatial separations. It is important to note that the amplitudes of the 2-day W2 wave in the *Y* component are almost unaffected by the geomagnetic storms, particularly those in the NH. Only the last peak in the SH global 2-day wave is influenced by the geomagnetic storm. Therefore the 2-day wave response of the *Y* component could be almost entirely attributed to the 2-day wave activity in the MLT region.

[28] The amplitudes of the global 2-day W2 wave in the *Z* component for both hemispheres are shown in the bottom row in Figure 10. The amplification of the global 2-day W2 wave is produced by both the geomagnetic disturbances and the 2-day wave activity in the MLT region. There are clear responses to the two geomagnetic storms (the peaks are

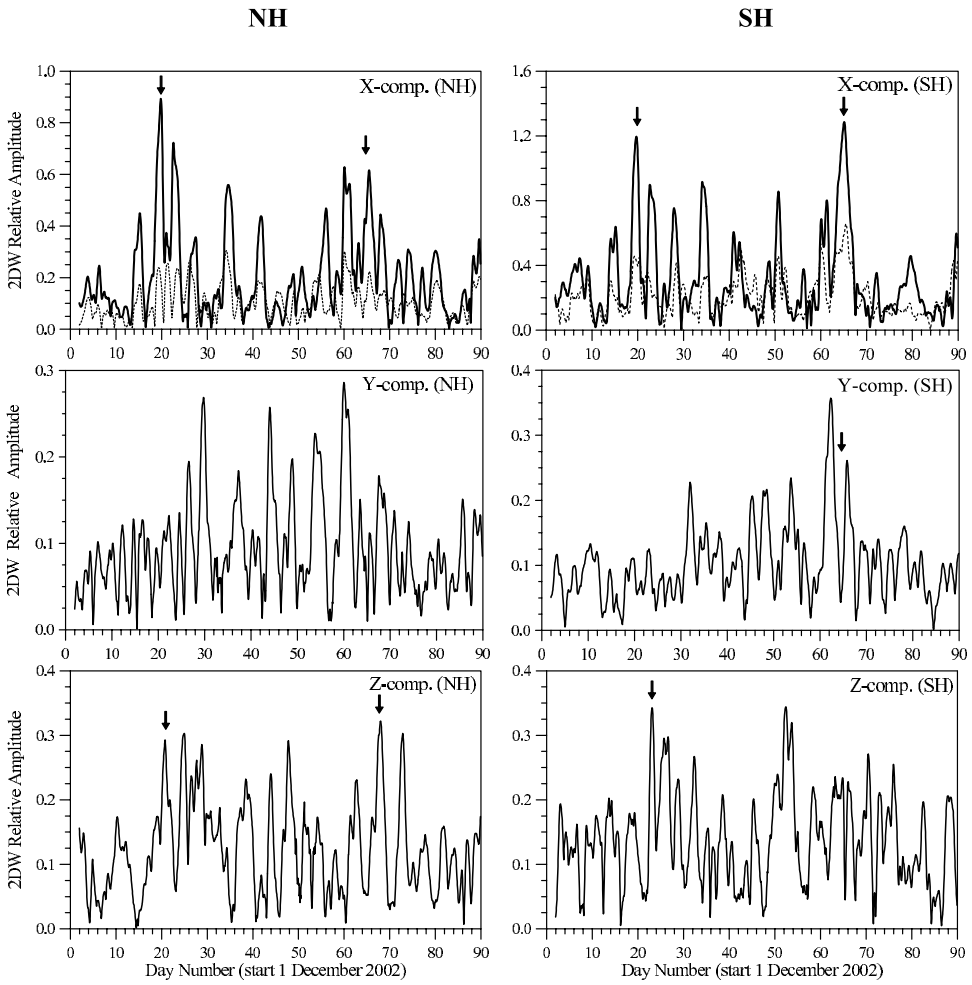

Figure 10. Amplitudes of global 2-day wave in all geomagnetic components obtained by a two-dimensional (time-longitude) Fourier transform for the NH (left column of plots) for the SH (right column of plots).

marked by arrows), but there are also significant peaks coinciding with the 2-day wave event in the MLT region (between day numbers 26 and 70). In this case, the wave amplitudes are quite large in both the initial and final stages of the 2-day wave activity.

4. A 2-Day Wave in the Maximum Electron Density of the Ionosphere F-region

[29] It was mentioned in section 1 that both the winds and the electric fields in the dynamo region produce plasma drifts that alter the distribution of the electron density in the ionosphere *F*-region. It is important also that near the magnetic equator where the geomagnetic field lines become horizontal, the dynamo electric fields generated by the global-scale waves play a leading role in the associated response of the ionosphere *F*-region. If we suppose that the obtained 2-day wave response of the geomagnetic components is caused mainly by the 2-day variability of the dynamo electric fields, then the 2-day variability could be transferred to the upper ionosphere by the produced plasma drifts. This intrinsic sensitivity of the upper ionosphere

Table 3. Geographic and Geomagnetic Coordinates of the Ionosonde Stations and Periods of Measurements

Stations	GGLAT	GGLONG	GMLAT	GMLONG	Period of Measurements
Grahamstown	−33.30	26.50	−34.28	91.6	01 Dec–28 Feb
Louisvale	−28.50	21.20	−28.61	87.6	01 Dec–28 Feb
Norfolk Island	−29.00	168.00	−33.85	246.2	21 Jan–27 Feb
Townsville	−19.30	146.70	−27.47	222.0	21 Jan–28 Feb
Ascension Island	−7.90	345.60	−2.12	57.1	01 Dec–28 Feb
Vanimo	−2.70	141.30	−11.61	214.4	21 Jan–27 Feb
Sao Luis	−2.50	315.80	+6.96	28.3	01 Dec–28 Feb

response to the electric fields induced by neutral winds in the low latitudes was taken into consideration in our further analysis.

[30] In order to study this problem we analyze the variability of the parameter *foF2* (the critical frequency of the ionosphere *F2*-layer) representing the maximum electron density of the *F*-region. We used hourly *foF2* data for seven tropical ionosonde stations, as data for six of them are obtained from the WDC, Boulder. The selected stations are listed in Table 3 together with their geographic and geomagnetic coordinates along with the periods of available data. All these ionosonde stations are situated in the SH and three of them (the Australian stations) have measurements only during the second part of the period of interest, i.e., after 21 January. Figure 11 shows the wavelet spectra calculated for the period of 36–96 hours for all stations. Clear peaks for periods near 48 hours between day numbers 50–60 are present at all stations. This 2-day oscillation in *foF2* coincides with the second interval of the 2-day wave amplification in the *Y* and *Z* components observed in the final stage of the 2-day wave activity in the MLT region. The mean amplitude of the 2-day oscillation in *foF2* was about 1.1–1.5 MHz (only the 2-day wave peak at Ascension Island was larger than 2 MHz, but this could partly be attributed to the data quality). Three of the ionosonde stations made measurements during the first interval of the 2-day wave amplifications in the *Y* and *Z* components observed in late December and early January and two of them, Sao Luis and Grahamstown, revealed clear 2-day variations in early January. At the same time the Louisvale station showed only a very weak signature of such an oscillation.

[31] The wavelet transform helped us to solve only the first part of the problem: the detection of 2-day variations in *foF2*. We need to examine these variations in detail in order to determine whether they are fluctuations due to other sources or they represent a zonally propagating wave. For this purpose we employ the same method applied to the geomagnetic data and described in detail in section 3.1. Only the period of 20 January to 1 February is analyzed, during which clear 2-day variations were found in all ionosonde stations. As in the analysis of the geomagnetic data, a vector averaging of the amplitudes and phases was performed to obtain the mean amplitude and phase of the 2-day wave for each station from 20 January to 1 February. The seven stations considered are longitudinally distributed in the SH enabling a study of the zonal structure of the 2-day variations observed in the maximum electron density of the ionosphere *F* region. Figure 12 shows the phase slope found in the relative scale coefficients of *foF2* for all stations. The longitudinal distribution of phases for *foF2* reveals a westward propagating 2-day W2 wave response of the ionosphere.

5. Discussion and Summary

[32] The main focus of this work was to study the vertical coupling of the low-latitude atmosphere-ionosphere system accompanying the quasi-2-day wave observed in the tropical MLT region. The problem was studied from an observational point of view, and three types of data were analyzed for this purpose. The 2-day wave event in the period from 1 December 2002 to 28 February 2003 was identified in neutral winds by radar measurements located at four tropical stations (Table 1). The 2-day variations in ionospheric electric currents (registered by perturbations in the geomagnetic field) and in *F*-region electron densities were detected in data from 23 magnetometer (Table 2) and seven ionosonde stations (Table 3) situated at low latitudes. The goal was to look for similarities between the 2-day wave in MLT winds and the 2-day variability in geomagnetic fields and in the *foF2* in order to reveal correlations between these variables. We investigated in detail two features for each kind of data: the variation with time of amplitude and zonal wave number. The results from observations can be summarized as follows:

[33] 1. A burst-like 2-day wave activity prevailed in the tropical MLT region having the following features: (1) the 2-day wave appeared in late December (around 25 December), peaked at most of the stations between 10 and 25 January, and persisted until early February (it disappeared around day number 70); however, no coherent amplification of the bursts was observed, (2) westward propagation of the 2-day wave, but with no single wave number found (it was apparently a combination of W2 and W3); large latitudinal gradient of phases and phase variability because of coupling between the 2-day wave and the longer-period 6–8-day wave, hampered the wave number determination, (3) vertical wavelengths were quite similar for all stations, ~50 to 65 km, and (4) the 2-day wave appeared to penetrate into the dynamo region for part of the time (predominantly after 20 January).

[34] 2. Simultaneous magnetometer data from a large number of stations in the tropical zone revealed (1) the 2-day variability in the geomagnetic components appeared as modulations of the quiet-day *Sq* diurnal cycle; this observational evidence was used as a basis for suggesting a novel method of data analysis, (2) the 2-day wave response in the *X* component was overwhelmed by two geomagnetic disturbances and was determined to be a W1 wave, (3) the 2-day wave responses of the *Y* and *Z* components coincided mainly with the 2-day wave event in the MLT region, however, the amplitudes were the greatest at the initial and final stages of the 2-day wave event, when the amplitudes of the 2-day wave itself were not as strong; some influence of the geomagnetic storms, particularly on the *Z* component response, was also present, (3) the 2-day wave response of the *Y* and *Z* component was determined to be a W2 wave.

[35] 3. Simultaneous ionosonde data from seven tropical stations indicated a 2-day wave response in *foF2* determined to be a W2 wave.

[36] To infer that the 2-day wave responses of the *Y* and *Z* components were forced directly by the 2-day wave penetrating into the dynamo region, we must demonstrate some similarity in the wave amplitudes and the same zonal structure for both 2-day wave events. The requirement for the same zonal structure is not completely fulfilled but also not rejected as both 2-day wave events propagate westward, and for at least part of the time W2 best described the 2-day wave in the neutral winds. However, the amplification of the 2-day wave response in the *Y* and *Z* components in late December and early January as well as in late January and early February, at times when the 2-day wave itself was not

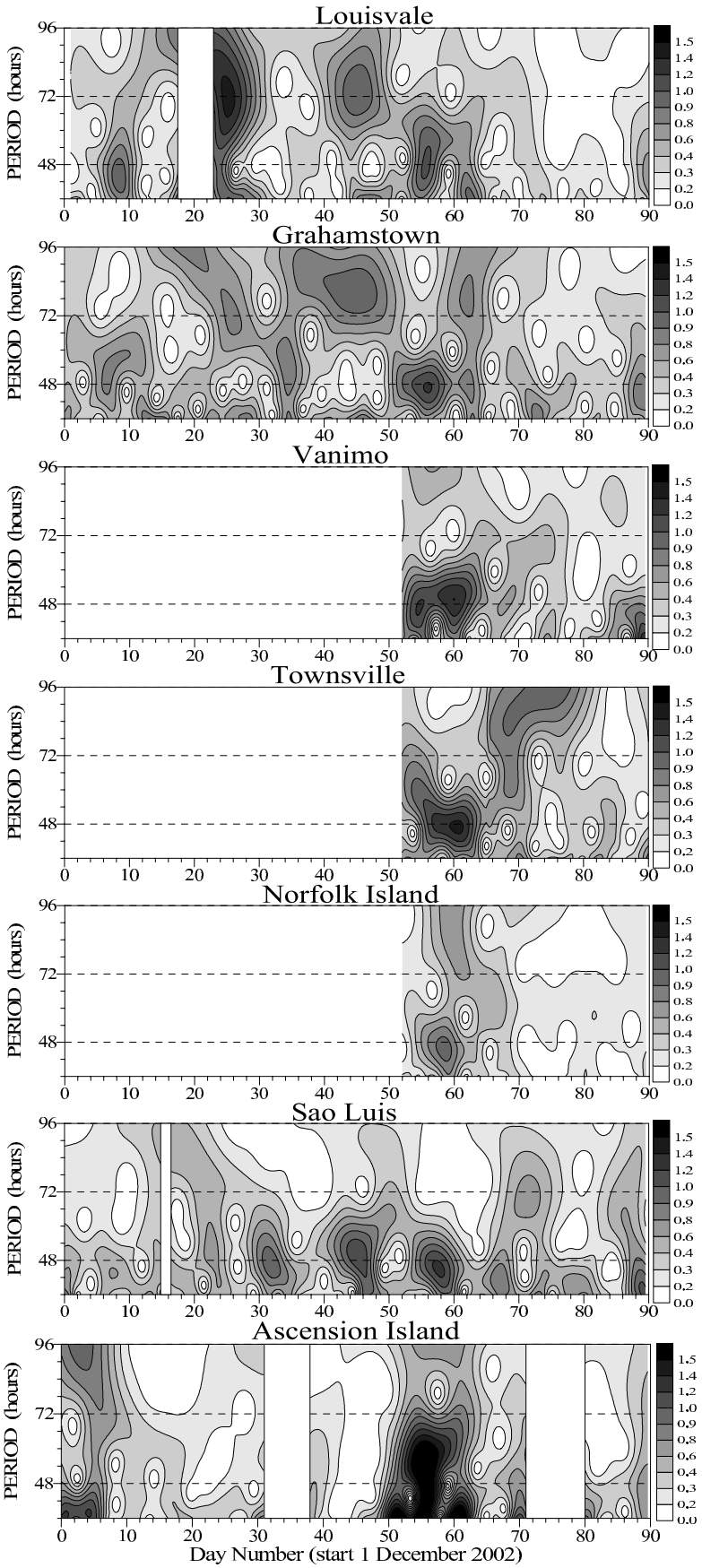

Figure 11. Wavelet spectra calculated from the hourly *foF2* data for the period range 36–96 hours for the seven ionosonde stations.

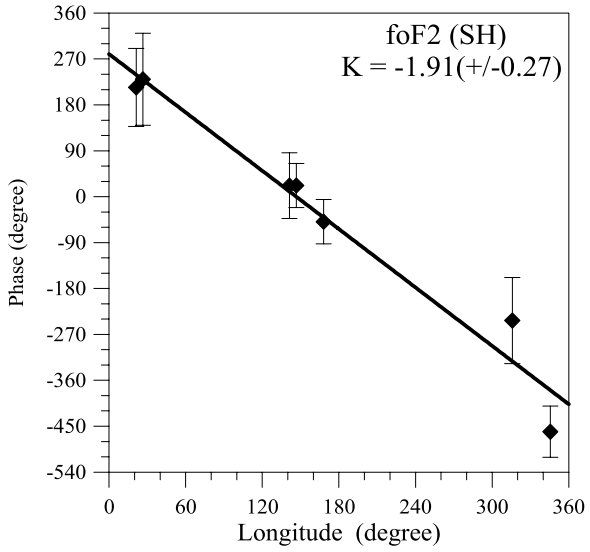

Figure 12. Phase slope found in the relative scale coefficients of *foF2* for the period of 20 January to 1 February 2003.

strong does not appear to require the direct involvement of the 2-day wave in the vertical coupling (or at least not during the entire period).

[37] The dynamics of the MLT region, however, can affect the ionosphere dynamo by modulated tides that penetrate deeply into the dynamo region. *Pancheva* [2006] investigated in detail the 2-day wave/tidal coupling (both for diurnal and semidiurnal tides) observed over Ascension Island at the end of January and the beginning of February, at the final stage of the 2-day wave activity. The coupling occurred when the 2-day wave period differed from 48 hours, phases were stable, and amplitudes were not as large as in the preceding very strong 2-day wave bursts. The author found evidence supporting the validity of a nonlinear interaction as a mechanism responsible for the observed 2-day tidal modulations in the equatorial MLT region during January/February 2003. This finding stimulated additional interest in the influences of tidal variability. To study the 2-day variability of the 24- and 12-hour tidal amplitudes, we applied the same procedure for analysis of wind data as used by *Pancheva* [2006]. A Morlet wavelet transform was performed on the hourly tidal amplitudes calculated for periods between 30 and 96 hours. The wavelet spectra of the 24-hour tidal amplitudes for all stations are shown in the left column in Figure 13, while those of the 12-hour tidal amplitudes are shown in the right column. The 2-day tidal modulations are clearly outlined at the initial (end of December and early January) and final (end of January and early of February) stages of the 2-day wave activity that coincide to a great extent with the amplification of the 2-day wave response of the *Y* and *Z* components. There are also secondary bursts of 2-day tidal modulations observed between day numbers 40 and 50 for the 24-hour tidal amplitudes and for the 12-hour tidal amplitudes near day

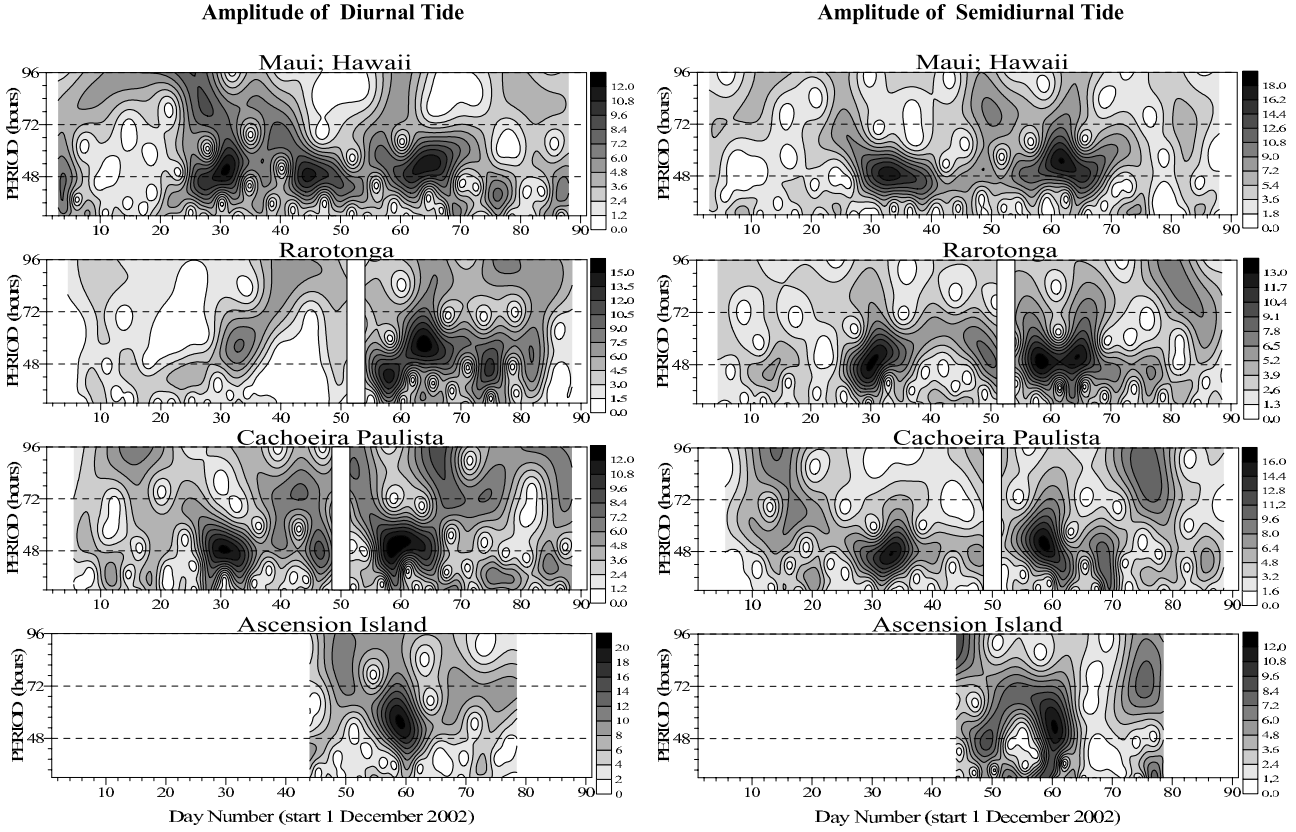

Figure 13. Wavelet spectra of 24-hour tidal amplitudes (left column) and 12-hour tidal amplitudes (right column) calculated in the period range 30–96 hours for all stations.

number 50. Careful inspection shows that there is a good correspondence between these secondary bursts of modulated tides and the peaks of the geomagnetic field variations at 2-day period (in the *Y* and *Z* components).

[38] It is worth noting that the 2-day modulation of the 24-hour tidal amplitude at the initial and final stages of the 2-day wave activity is probably due to the observed anti-correlation between the 2-day wave activity and the diurnal tide [*Harris and Vincent*, 1993; *Gurubaran et al.*, 2001a, 2001b; *Pancheva et al.*, 2004a, 2004b]. The 24-hour tide was still sufficiently strong at the initial and final stages of the 2-day wave activity to interact effectively with the 2-day wave and to yield secondary waves [*Pancheva*, 2006]. This means that significant tidal modulations, such as those observed in Figure 13, can be produced by tides having at least moderate amplitudes.

[39] The results shown in Figure 13 suggest that the 2-day modulated tides (diurnal and semidiurnal) most probably have more significant effects on the dynamo region than only the direct penetration of the 2-day wave. The atmospheric tides, and particularly the semidiurnal tide, propagate freely upward in the thermosphere and then participate in the dynamo generation of electric fields at higher levels. If the tidal amplitudes are strongly modulated with a period of 2 days, they can induce a 2-day variability of the electric fields as well. It should be noted that the 2-day modulated semidiurnal tide might be more effective in producing a 2-day variability of the electric fields than the modulated diurnal tide because usually the vertical wavelength of the semidiurnal tide is significantly larger than that of the diurnal tide. It is worth mentioning also that a combined effect of the 2-day wave with the modulated tides most probably produced so strong 2-day variability of the geomagnetic components as those shown in Figure 6. An important question is what kind of relationship between the 2-day wave and the tides should exist in order for their combined action to produce a 2-day variability of the current vortex.

[40] The ionosphere F-region response at low latitudes is very sensitive to the dynamo generated electric fields because of the special geometry of the magnetic field. In this case the 2-day variability of the electric fields generated by the modulated tides or by combined effect of the 2-day wave with the modulated tides is easily transferred to the upper ionosphere by producing 2-day variability of the vertical plasma drift. This variable plasma drift then generates 2-day variability in the maximum electron density of the *F*-region.

[41] In conclusion, we note that the global 2-day W2 wave seen in the ionospheric currents and in the *F*-region plasma is forced by the simultaneous 2-day wave activity in the MLT region. The main forcing agent in this atmosphere-ionosphere coupling seems to be the modulated tides, particularly the 12-hour tide which has a vertical wavelength larger than the 24-hour tide and propagates deeply into the thermosphere. Further, some direct effect of the MLT 2-day wave on the dynamo region cannot be excluded. The parameter that appears to be affected, and thus drives the observed 2-day wave response of the ionosphere, is the dynamo electric field. We note that the planetary waves may have some effect on the collision frequency through composition changes at turbopause and hence influence the conductivity at higher altitudes, but most probably this effect is of secondary importance.

[42] **Acknowledgments.** This work was supported by INTAS grant 03-51-6425. Operational support for the Rarotonga MF radar was provided under NASA contract NMH05CC70C. The authors gratefully acknowledge the work of the World Data Centre for Geomagnetism, Denmark and World Data Centre, Boulder for data access and availability. One of the authors, DP, is grateful for enlightening discussions with A. Richmond, R. Lieberman, and C. Haldoupis on the dynamics and electrodynamics of low latitudes. We wish to thank also to two anonymous reviewers for their comments on the original manuscript.

[43] Zuyin Pu thanks S. Gurubaran and Jan Lastovicka for their assistance in evaluating this paper.

References

Abdu, M. A., T. K. Ramkumar, I. S. Batista, C. G. Brum, H. Takahashi, B. W. Reinisch, and I. H. Sobra (2006), Planetary wave signatures in the equatorial atmosphere-ionosphere system and mesosphere, E- and F-region coupling, *J. Atmos. Sol. Terr. Phys.*, *68*, 509–522.

Altadill, D., and E. Apostolov (1998), Vertical development of the 2-day wave in the midlatitude ionospheric F-region, *J. Geophys. Res.*, *103*, 29,199–29,206.

Apostolov, E. M., D. Altadill, and L. F. Alberca (1995), Characteristics of quasi-2-day oscillations in the foF2 at northern middle latitude, *J. Geophys. Res.*, *100*, 12,163–12,171.

Blanc, M., and A. D. Richmond (1980), The ionospheric disturbance dynamo, *J. Geophys. Res.*, *85*, 1669–1686.

Bloomfield, P. (1976), *Fourier Analysis of Time Series: An Introduction*, John Wiley, Hoboken, N. J.

Chen, P.-R. (1992), Two day oscillation of the equatorial ionization anomaly, *J. Geophys. Res.*, *97*, 6343–6357.

Forbes, J. M., and S. Leveroni (1992), Quasi 16-day oscillation in the ionosphere, *Geophys. Res. Lett.*, *19*, 981–984.

Forbes, J. M., R. Guffe, X. Zang, D. Fritts, D. Riggin, A. Manson, C. Meek, and R. Vincent (1997), Quasi-2-day oscillation of the ionosphere during summer 1992, *J. Geophys. Res.*, *102*, 7301–7305.

Gurubaran, S., T. K. Ramkumar, S. Sridharan, and R. Rajaran (2001a), Signatures of quasi-2-day planetary waves in the equatorial electrojet: results from simultaneous observations of mesospheric winds and geomagnetic field variations at low latitudes, *J. Atmos. Sol. Terr. Phys.*, *63*, 813–821.

Gurubaran, S., S. Sridharan, T. K. Ramkumar, and R. Rajaram (2001b), The mesospheric quasi-2-day wave over Tirunelveli (8.7°N), *J. Atmos. Sol. Terr. Phys.*, *63*, 975–985.

Hagan, M. E., J. M. Forbes, and F. Vial (1993), Numerical investigation of the propagation of the quasi-2-day wave into the lower thermosphere, *J. Geophys. Res.*, *98*, 23,193–23,205.

Harris, T. J., and R. A. Vincent (1993), The quasi-2-day wave observed in the equatorial middle atmosphere, *J. Geophys. Res.*, *98*, 10,481–10,490.

Ito, R., S. Kato, and T. Tsuda (1986), Consideration of an ionospheric wind dynamo driven by a planetary wave with a two-day period, *J. Atmos. Terr. Phys.*, *48*, 1–13.

Kikuchi, T., H. Lühr, T. Kitamura, O. Saka, and K. Schlegel (1996), Direct penetration of the polar electric field to the equator during a DP 2 event as detected by the auroral and equatorial magnetometer chains and the EISCAT radar, *J. Geophys. Res.*, *101*, 17,161–17,173.

Lastovicka, J. (2006), Forcing of the ionosphere by waves from below, *J. Atmos. Sol. Terr. Phys.*, *68*, 479–497.

Nishida, A. (1968), Coherence of geomagnetic DP2 fluctuations with interplanetary magnetic variations, *J. Geophys. Res.*, *73*, 5549.

Pancheva, D. (2006), Quasi-2-day wave and tidal variability observed over Ascension Island during January/February 2003, *J. Atmos. Sol. Terr. Phys.*, *68*, 390–407.

Pancheva, D., and I. Lysenko (1988), Quasi-2-day fluctuations observed in the summer F region electron maximum, *Bulg. Geophys. J.*, *14*, 41–51.

Pancheva, D., L. F. Alberca, and B. de la Morena (1994), Simultaneous observation of the quasi-2-day wave in the lower and upper ionosphere over Europe, *J. Atmos. Terr. Phys.*, *56*, 43–50.

Pancheva, D., et al. (2004a), Variability of the quasi-2-day wave observed in the MLT region during the PSMOS campaign of June–August 1999, *J. Atmos. Sol. Terr. Phys.*, *66*, 539–565.

Pancheva, D., N. J. Mitchell, and P. T. Younger (2004b), Meteor radar observations of atmospheric waves in the equatorial mesosphere/lower thermosphere over Ascension Island, *Ann. Geophys.*, *22*, 387–404.

Parish, H. F., J. M. Forbes, and F. Kamalabadi (1994), Planetary wave and solar emission signatures in the equatorial electrojet, *J. Geophys. Res.*, *99*, 355–368.

Parkinson, W. D. (1982), Bi-diurnal geomagnetic variations, *Ann. Geophys.*, *38*, 327–329.

Ramkumar, T. K., Y. Bhavanikumar, D. Narayana Rao, S. Gurubaran, A. Narendra Badu, A. K. Ghosh, and R. Rajaram (2005), Observational evidences on the influences of tropical lower atmospheric ~20 day oscillation on the ionospheric equatorial electrojet, *J. Atmos. Sol. Terr. Phys.*, *68*, 523–538.

Rangarajan, G. K. (1994), Quasi-bidaily variation of the geomagnetic field in the Indian Equatorial Zone, *J. Geomagn. Geoelectr.*, *46*, 373–380.

Richmond, A. (1995), The ionospheric wind dynamo: effects of its coupling with different atmospheric regions, in *The Upper Mesosphere and Lower Thermosphere: A Review of Experiment and Theory*, *Geophys. Monogr. Ser.*, vol. 87, edited by R. M. Johnson and T. L. Killeen, pp. 49–65, AGU, Washington, D. C.

Takahashi, H., L. M. Lima, M. A. Abdu, I. S. Batista, D. Gobi, R. A. Buriti, and P. P. Batista (2005), Evidence on 2–4 day oscillations of the equatorial h′F and mesospheric airglow emissions, *Geophys. Res. Lett.*, *32*, L12102, doi:10.1029/2004GL022318.

Takeda, M., and Y. Yamada (1989), Quasi two-day period variations of the geomagnetic field, *J. Geomagn. Geoelectr.*, *41*, 469–478.

Takeda, M., T. Iyemori, and A. Saito (2003), Relationship between electric field and currents in the ionosphere and the geomagnetic Sq field, *J. Geophys. Res.*, *108*(A5), 1183, doi:10.1029/2002JA009659.

Yamada, Y. (2002), 2-day, 3-day and 5–6-day oscillations of the geomagnetic field detected by principal component analysis, *Earth Planets Space*, *54*, 379–392.

M. A. Abdu, I. S. Batista, P. P. Batista, and B. R. Clemesha, National Center for Space Research, São José dos Campos, 12245-970 Sao Paolo, Brazil.

S. J. Franke, Department of Electrical and Computer Engineering, University of Illinois at Urbana-Champaign, 1308 W. Main Street, Urbana, IL 61802, USA.

D. C. Fritts and D. M. Riggin, Colorado Research Associates, Division of NorthWest Research Associates, 3380 Mitchell Lane, Boulder, CO 80301, USA.

T. Kikuchi, Solar-Terrestrial Environment Laboratory, Nagoya University, Honohara 3-13, Toyokawa, Aichi 442-8507, Japan.

N. J. Mitchell and D. V. Pancheva, Centre for Space, Atmosphere, and Oceanic Science, Department of Electronic and Electrical Engineering, University of Bath, Bath BA2 7AY, UK. (eesdvp@bath.ac.uk)

P. J. Mukhtarov, Geophysical Institute, Bulgarian Academy of Sciences, 3 Acad. G. Bonchev Street, 1113 Sofia, Bulgaria.

M. G. Shepherd, Centre for Research in Earth and Space Science, York University, 4700 Keele Street, Toronto, Ontario, M3J 1P3 Canada.